



Article

Methods for Obtaining One Single Larmor Frequency, Either ν_1 or ν_2 , in the Coherent Spin Dynamics of Colloidal Quantum Dots

Meizhen Jiang ^{1,†}, Yuanyuan Zhang ^{1,†}, Rongrong Hu ^{2,*}, Yumeng Men ¹, Lin Cheng ¹, Pan Liang ³, Tianqing Jia ¹, Zhenrong Sun ¹ and Donghai Feng ^{1,4,*}

¹ State Key Laboratory of Precision Spectroscopy, East China Normal University, Shanghai 200241, China; 52200920010@stu.ecnu.edu.cn (M.J.); 52170920029@stu.ecnu.edu.cn (Y.Z.); 52250920010@stu.ecnu.edu.cn (Y.M.); 51210920033@stu.ecnu.edu.cn (L.C.); tqjia@phy.ecnu.edu.cn (T.J.); zrsun@phy.ecnu.edu.cn (Z.S.)

² College of Sciences, Shanghai Institute of Technology, Shanghai 201418, China

³ College of Arts and Sciences, Shanghai Dianji University, Shanghai 201306, China; liangp@sdju.edu.cn

⁴ Collaborative Innovation Center of Extreme Optics, Shanxi University, Taiyuan 030006, China

* Correspondence: hrr92@sit.edu.cn (R.H.); dhfeng@phy.ecnu.edu.cn (D.F.)

† These authors contributed equally to this work.

Abstract: The coexistence of two spin components with different Larmor frequencies in colloidal CdSe and CdS quantum dots (QDs) leads to the entanglement of spin signals, complicating the analysis of dynamic processes and hampering practical applications. Here, we explored several methods, including varying the types of hole acceptors, air or anaerobic atmosphere and laser repetition rates, in order to facilitate the obtention of one single Larmor frequency in the coherent spin dynamics using time-resolved ellipticity spectroscopy at room temperature. In an air or nitrogen atmosphere, manipulating the photocharging processes by applying different types of hole acceptors, e.g., Li[Et₃BH] and 1-octanethiol (OT), can lead to pure spin components with one single Larmor frequency. For as-grown QDs, low laser repetition rates favor the generation of the higher Larmor frequency spin component individually, while the lower Larmor frequency spin component can be enhanced by increasing the laser repetition rates. We hope that the explored methods can inspire further investigations of spin dynamics and related photophysical processes in colloidal nanostructures.

Keywords: colloidal quantum dots; spin dynamics; time-resolved spectroscopy; hole acceptors



Citation: Jiang, M.; Zhang, Y.; Hu, R.; Men, Y.; Cheng, L.; Liang, P.; Jia, T.; Sun, Z.; Feng, D. Methods for Obtaining One Single Larmor Frequency, Either ν_1 or ν_2 , in the Coherent Spin Dynamics of Colloidal Quantum Dots. *Nanomaterials* **2023**, *13*, 2006. <https://doi.org/10.3390/nano13132006>

Academic Editor: Wolfgang Heiss

Received: 3 June 2023

Revised: 2 July 2023

Accepted: 3 July 2023

Published: 5 July 2023



Copyright: © 2023 by the authors. Licensee MDPI, Basel, Switzerland. This article is an open access article distributed under the terms and conditions of the Creative Commons Attribution (CC BY) license (<https://creativecommons.org/licenses/by/4.0/>).

1. Introduction

The electron spin in semiconductors is a promising candidate for quantum bits which are the elementary units for quantum information processing [1–3]. It is of fundamental importance to understand electron spin properties and further control the spins. Compared with bulk semiconductors, the confined electrons in quantum dots (QDs) are more adaptable to quantum information science, due to the less efficient spin–orbit interaction and longer spin dephasing times [4]. Over the past two decades, many efforts have been dedicated to investigating the spin properties and the spin manipulation in colloidal QDs grown using wet chemical approaches, obtaining long spin dephasing times up to few nanoseconds even at room temperature [5–7]. The open surface and surrounding matrix of colloidal QDs provide convenience for optical and chemical manipulation of electron spin [8–12]. In addition, colloidal QDs have the advantages of low cost and easily controlled shapes, sizes and structures. Since it was first reported by J. A. Gupta et al. that ensembles of colloidal CdSe QDs show two distinct spin components in the coherent dynamics, which differ in *g* factors and Larmor frequencies [13], colloidal CdS QDs [10] were also found to have similar phenomena. The coexistence of two spin components with different Larmor frequencies (referred to below as ν_1 and ν_2) entangles the spin signals and complicates the investigation of their origins and the related spin relaxation mechanisms.

For instance, in ensembles of colloidal CdSe QDs, the v_1 and v_2 spins with spin dephasing times up to hundreds of picoseconds were assigned to the electron and exciton, respectively (electron–exciton model) [5], which is, however, contradictory to the fact that exciton spin relaxation times are short and have around a subpicosecond time scale [14]. Recently, the two spin components were redemonstrated to both belong to electrons in photocharged QDs, which have different wave function spreads, which were either confined by the QD potential (corresponding to the v_1 component) or additionally localized in the surface vicinity (corresponding to the v_2 component) [11]. Similarly, for CdSe nanocrystals embedded in a glass matrix, a solely detected Larmor precession frequency (corresponding to the v_2 component in solution-grown colloidal CdSe QDs) was also determined to arise from resident electrons localized in the vicinity of the surface [15]. However, a systematic investigation of separation and manipulation of the two spin components is still lacking. Obtaining one pure spin component is not only important for deeper understanding of the underlining spin relaxation mechanism and related photophysics but also crucial for the practical applications of quantum bits.

In this work, we investigated the spin signals of colloidal CdSe and CdS QDs in toluene using time-resolved ellipticity spectroscopy under different photocharging conditions, such as addition of different types of hole acceptors, changing laser repetitions as well as air and nitrogen (N_2) atmospheres. We systematically studied the methods that can contribute to obtaining or enhancing one single Larmor frequency, either v_1 or v_2 , in the coherent spin dynamics. In a N_2 atmosphere, the addition of hole acceptor, either Li[Et₃BH] or 1-octanethiol (OT), is beneficial to obtain the spin signal of the v_1 component, while adding the OT hole acceptor in an air atmosphere usually brings the v_2 spin component into being separately. High laser repetition rates can enhance the spin signal of the v_1 component, whereas low laser repetition rates are convenient for obtaining the v_2 component alone.

2. Materials and Methods

2.1. Sample Preparation

Octadecylamine-stabilized colloidal CdSe (average diameter: 6.5 nm, estimated from the first exciton absorption peak [16]) and oleic-acid-stabilized CdS QDs (average diameter: 5.3 nm) in toluene solution were commercially obtained from Hangzhou Najing Technology Co., Ltd. (Hangzhou, China) The corresponding absorption spectra are shown in Figure 1. The mass concentration of all obtained QD samples is 5 mg/mL. For photocharging experiments, the well-known OT hole acceptor [17] or Li[Et₃BH] [18], purchased from Sigma Aldrich, was mixed with toluene solutions of CdSe or CdS QDs in an airtight quartz cuvette with a thickness of 1 mm. For Li[Et₃BH], the sample preparation was performed in a glove box in a N_2 atmosphere. The OT hole acceptor was mixed with QDs in either a N_2 or air atmosphere. The final concentrations of all samples in the measurements were kept the same at 2.5 mg/mL.

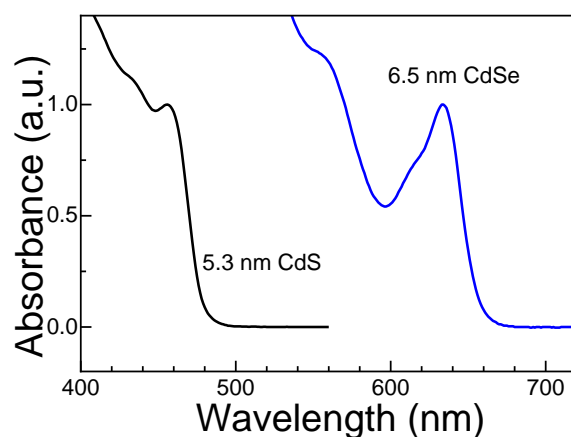


Figure 1. Absorption spectra of as-grown colloidal 6.5 nm CdSe and 5.3 nm CdS QDs. The intensity of the first absorption peak of CdSe and CdS QDs is normalized.

2.2. Setup for the Measurements of Coherent Electron Spin Dynamics

The coherent spin dynamics of colloidal QDs were measured using time-resolved ellipticity spectroscopy [11,19,20]. The experimental configuration depicted in Figure 2 is based on a ytterbium-doped potassium gadolinium tungstate (Yb-KGW) regenerative amplifier (PHAROS, Light Conversion Ltd; the central wavelength is 1026 nm, and the pulse duration is ~270 fs), combined with an optical parametric amplifier (OPA). The laser repetition rates of the OPA outputs are tunable and up to 50 kHz. All the measurements were performed at room temperature and in a transverse external magnetic field provided by an electromagnet with iron poles.

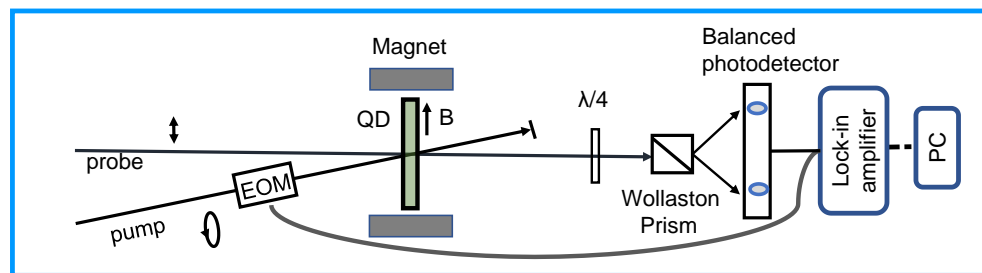


Figure 2. Setup schematic of time-resolved ellipticity measurements.

In the pump–probe measurements as shown in Figure 2, the pump and probe pulses are wavelength-degenerate and emitted from the OPA with their wavelength tuned at the low energy side of the first exciton absorption band. The circularly polarized pump pulses generate the spin polarization in the QD samples, while the subsequent dynamics of this spin polarization are monitored by the change of ellipticity of the linearly polarized probe pulses. The linearly polarized probe pulses become partially elliptically polarized after transmitting through the spin-polarized QDs because of the absorption difference of left- and right-circularly polarized light. The time delay between the pump and probe pulses is adjusted by a mechanical delay line.

3. Results

3.1. Spin Dynamics of As-Grown CdSe and CdS Colloidal QDs with Native Ligands

As-grown colloidal CdSe and CdS QDs with native ligands normally have two spin Larmor frequencies in coherent spin dynamics measured at high laser repetition rates. As shown in Figure 3, time-resolved ellipticity signals of as-grown colloidal CdSe and CdS QDs are measured in a transverse magnetic field B of 500 and 300 mT, respectively. The corresponding fast Fourier transform (FFT) spectra are shown in the right panels of Figure 3. Figure 3c is the fast Fourier transform (FFT) spectrum of the spin dynamics of CdSe QDs, which shows two Larmor precession frequencies of $\nu_1 = 7.32$ GHz and $\nu_2 = 11.11$ GHz. Two g factor values of $g_1 = 1.05$ and $g_2 = 1.59$ are correspondingly derived from these frequencies by the equation $g = h\nu_L / (\mu_B B)$, where h , ν_L and μ_B are the Planck constant, Larmor precession frequency and Bohr magneton, respectively. Both g factor values are in line with the size dependence of g factors reported in the literature [11]. Similarly, Figure 3d shows two Larmor precession frequencies and the corresponding g factors of CdS QDs of $\nu_1 = 7.73$ GHz, $g_1 = 1.85$, and $\nu_2 = 8.12$ GHz, $g_2 = 1.93$. Despite the FFT amplitudes and spin dynamic curves of CdSe and CdS QDs being distinctly different, both the spin signals comprise two Larmor frequencies (the smaller one refers to the ν_1 component, and the larger one is the ν_2 component). The FFT amplitude of the ν_1 component is much smaller than that of the ν_2 component in CdSe QDs, while it is the opposite in CdS QDs. The difference of relative FFT amplitudes may result from different surface ligands and their interactions with the QDs. It has been shown in the literature that the ν_1 component is stronger than the ν_2 component for as-grown 6 nm CdSe QDs with stearic acid stabilizing ligands [21], while the ν_1 component is significantly weaker than the ν_2 component for 6.1 nm CdSe QDs with octadecylamine stabilizing ligands [22]. In the following, we will

provide appropriate methods which selectively bring one of the two spin components into being, or purposefully enhance one of them and suppress the other.

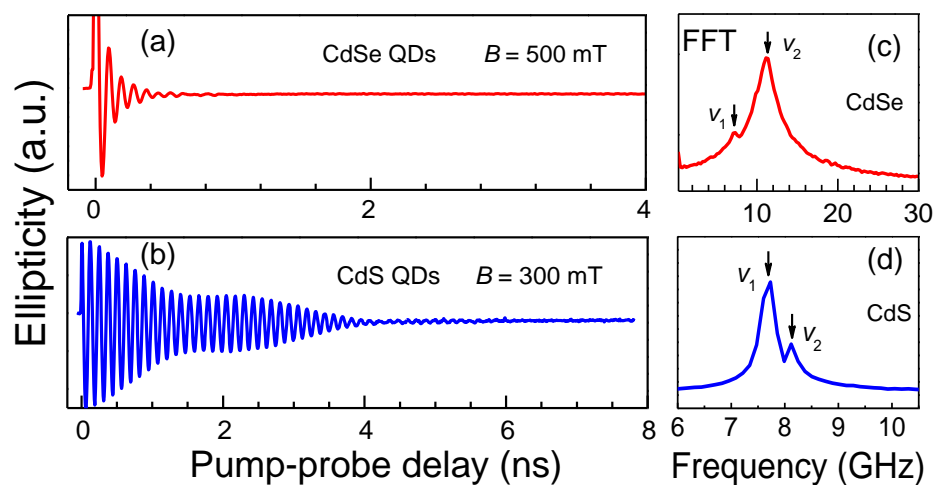


Figure 3. Time-resolved ellipticity signals in as-grown colloidal (a) CdSe and (b) CdS QDs. (c) and (d) are the fast Fourier transform (FFT) spectra of panel (a) and (b), respectively. The laser repetition rate is 50 kHz.

3.2. Methods to Individually Obtain the v_1 Component

Adding hole acceptors to the QD solutions is helpful in manipulating the spin signals. Figure 4a,b show time-resolved ellipticity signals in as-grown colloidal CdSe and CdS QDs and QDs with Li[Et₃BH] hole acceptors prepared in a N₂ atmosphere. The presence of the hole acceptor Li[Et₃BH] strongly increases the ellipticity signals both for CdSe and CdS QDs. As depicted in the insets of Figure 4a,b, actually only the v_1 component is remarkably enhanced, while the v_2 component disappears. This indicates that addition of Li[Et₃BH] hole acceptors in a N₂ atmosphere is conducive to separating the entangled spin signals by increasing the v_1 component and suppressing the v_2 component. The reason is that the Li[Et₃BH] hole acceptor, as a strong chemical reducing agent, can capture the photogenerated holes and leave the electrons in the dot core (corresponding to photocharging state of the v_1 component [11]). With enough Li[Et₃BH] molecules, all QDs could be charged to this state, and the spin signal of the v_2 component (which corresponds to another charging state [11]) is thus suppressed. With the removal of the influence of oxygen (as electron scavengers [23,24]) in a N₂ atmosphere, the photodoped electrons in the dot core are long-lived [18]. Under the irradiation of ambient room light and pump/probe pulses, the spin amplitudes of CdSe and CdS QDs with Li[Et₃BH] remain almost the same after two hours as shown in Figure 4c, indicating that stable photocharging can be obtained in CdSe and CdS QDs. Stable charging means that the generation of photocharging states can adequately compensate for their decay, which requires appropriate Li[Et₃BH] concentrations and appropriate light illumination conditions.

Consequently, an effective strategy to achieve pure states of the v_1 component is to modify colloidal QDs with Li[Et₃BH] hole acceptors in an anaerobic atmosphere. The spin signals of the v_1 component are considerably amplified, which also improves the signal-to-noise ratio significantly.

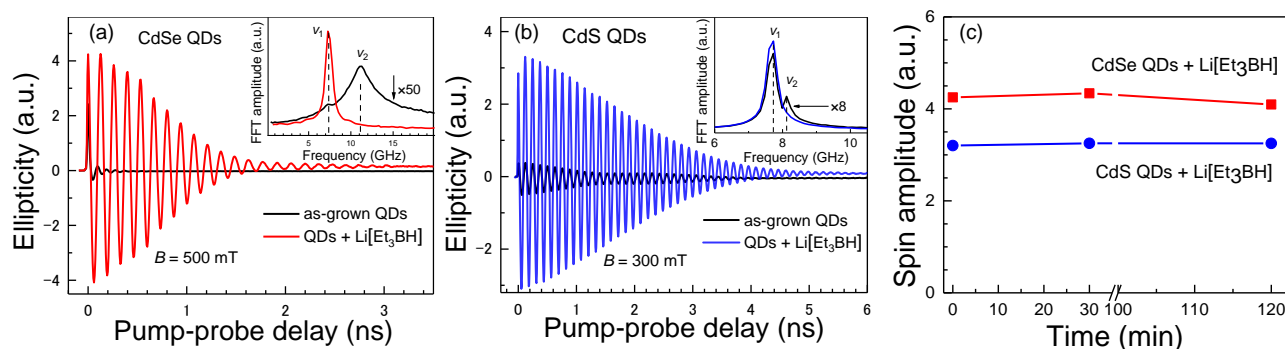


Figure 4. (a,b) Time-resolved ellipticity signals in as-grown colloidal CdSe and CdS QDs and QDs with Li[Et₃BH] prepared in a N₂ atmosphere. The insets are the corresponding FFT spectra of panel a and b. The FFT spectra of as-grown CdSe and CdS QDs are multiplied by 50 and 8, respectively, for better distinction of the two observed Larmor frequencies. (c) Spin amplitudes in CdSe and CdS QDs with Li[Et₃BH] as a function of time under ambient room light illumination. The molar ratio of Li[Et₃BH] to CdSe and CdS QDs is 500 and 10, respectively. The laser repetition rate is 50 kHz.

3.3. Methods to Individually Obtain the ν_2 Component

Inspired by the success of individually obtaining of the ν_1 spin component by modifying QDs surface with an appropriate hole acceptor in a N₂ atmosphere, we investigated the effect of adding another OT hole acceptor to QDs prepared in an air atmosphere. The comparison of the time-resolved ellipticity signals of CdSe QDs with and without OT prepared in an air atmosphere is shown in Figure 5a. Adding OT, the spin signal of the ν_2 component increases to about 8 times that of as-grown QDs. The inset of Figure 5a shows that the FFT amplitude of ν_2 enlarges, while ν_1 disappears. A similar phenomenon can be found in the measurements in as-grown CdS QDs and QDs with OT prepared in an air atmosphere, as depicted in Figure 5b. The spin amplitude of the ν_2 component significantly increases and brings the ν_2 component into being separately. Note that the laser repetition for CdS QDs with OT is 10 kHz. Since with the higher laser repetition, i.e., with 50 kHz laser repetition, the spin signal of the ν_1 component is apparent as a result of the pile-up effect from previous pulses. The ν_1 component can appear at high laser repetition rates, and the higher the laser repetition rate, the stronger the intensity of the ν_1 component, which will be illustrated below. For measurements with different laser repetition rates, a normalization of both pulse energies and laser powers is requisite. The spin signal of CdS QDs with OT measured at 10 kHz laser repetition rates in the main panel has already been multiplied by a factor of 5; equivalently, both the pulse energy and laser power are normalized to be the same between the measurements with 10 and 50 kHz laser repetition rates.

The following are possible reasons that account for the selective enhancement of the ν_2 spin component by using OT hole acceptors. OT molecules are linked to the QD surface by replacing native ligands and capture the photogenerated holes in QDs. Therefore, the captured holes are still in nearby the QD surface. Due to the Coulombic attraction, the electron also tends to stay at nearby the QD surface. This charging state contributes to the spin signal of the ν_2 component [11] and can be enhanced by addition of enough OT molecules. Meanwhile, the charging state corresponding to the ν_1 component is totally inhibited due to the presence of oxygen. Those results suggest that addition of OT with an appropriate molar ratio to QDs in an air atmosphere may provide an approach to obtaining the spin signal of the ν_2 component solely.

Note that modifying the QDs surface with an OT hole acceptor prepared in a N₂ atmosphere can also provide an effective strategy to boost the spin signal of the ν_1 component. The spin dynamics of CdSe QDs with and without an OT hole acceptor prepared in a N₂ atmosphere are shown in Figure 6a. Via adding OT, the total spin amplitudes of CdSe QDs are considerably enhanced. The FFT amplitudes of the ν_1 component are relatively weak in both as-grown CdSe QDs and QDs with OT (OT/QDs = 7000) compared with those of the

v_2 component as shown in Figure 6b. However, increasing the molar ratio of OT to QDs to 70,000, the FFT amplitude of the v_1 component is increased significantly, while the v_2 component is reduced. For CdS QDs, some similar phenomena also occur, e.g., addition of OT enhances the total spin signal, but some details are different. Figure 6c,d show the spin signals of colloidal CdS QDs and QDs with OT prepared in a N_2 atmosphere and the corresponding FFT spectra. When the molar ratio of OT to QDs is 100, there is only one frequency of the v_1 component, while the v_2 component disappears. However, increasing the molar ratio of OT to QDs to 5000, the v_2 component emerges again. The anaerobic conditions also help the enhancements of the v_1 component with addition of OT hole acceptors in both CdSe and CdS QDs. In some cases, with appropriate OT concentrations, even a pure v_1 spin component could be achieved.

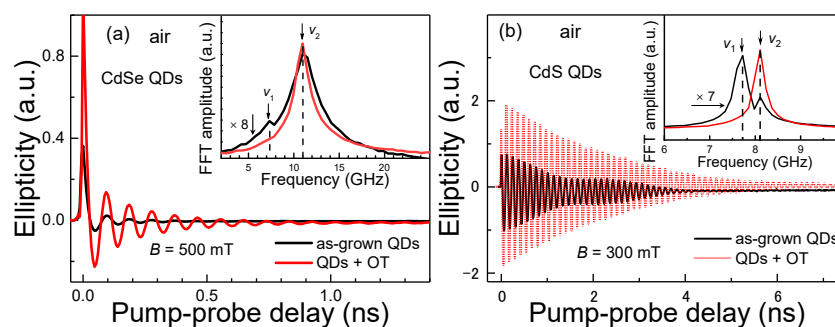


Figure 5. (a) Time-resolved ellipticity signals of as-grown colloidal CdSe QDs and QDs with 1-octanethiol (OT) prepared in an air atmosphere. The inset is the corresponding FFT spectra. The FFT spectroscopy of as-grown CdSe QDs is multiplied by 8 for clarity. The molar ratio of OT to CdSe QDs is 11,000. The laser repetition rate is 50 kHz. (b) Spin signals of as-grown colloidal CdS QDs and QDs with OT prepared in an air atmosphere. The inset is the corresponding FFT spectra. The FFT spectroscopy of as-grown CdS QDs is multiplied by 7 for clarity. The molar ratio of OT to CdS QDs is 5000. The laser repetition rates for as-grown CdS QDs and QDs with OT are 50 and 10 kHz, respectively.

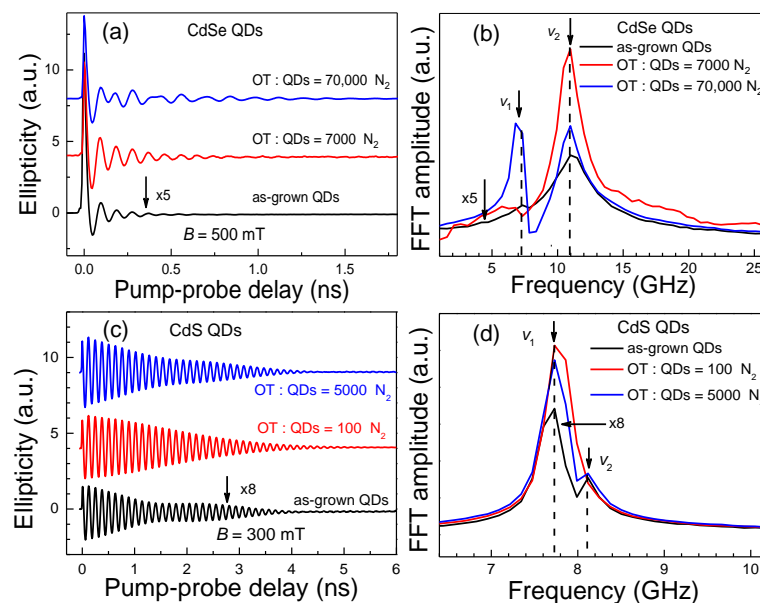


Figure 6. (a) Time-resolved ellipticity signals in as-grown colloidal CdSe QDs and QDs with OT prepared in a N_2 atmosphere. (b) The corresponding FFT spectra of panel a. The spin signal and its FFT spectroscopy of as-grown CdSe QDs are both multiplied by 5 for better clarity. The laser repetition rate is 50 kHz. (c) Spin signals of colloidal CdS QDs and QDs with OT prepared in a N_2 atmosphere. (d) The corresponding FFT spectra of panel c. The spin signal and its FFT spectroscopy of as-grown CdS QDs are both multiplied by 8. The laser repetition rate is 50 kHz. The plots in panel a and c are offset for clarity.

3.4. Influence of Laser Repetition Rates on Spin Signals

Figure 7 shows the spin dynamics of as-grown CdSe and CdS QDs (with native ligands at an air atmosphere) at different laser repetition rates and the corresponding FFT spectra. At a high laser repetition rate of 50 kHz, spin dynamics of colloidal QDs, either CdSe or CdS QDs, exhibit two distinct spin components with different Larmor precession frequencies, which is similar to the results shown in Figure 3. As the laser repetition rate decreases from 50 to 1 kHz, the spin amplitude reduces slightly, and the ν_1 component gradually disappears in CdSe QDs as shown in Figure 7a,b. At the laser repetition rate of 1 kHz, only the ν_2 component is shown in the coherent spin dynamics. The amplitudes of the ν_2 component show almost no change when altering the laser repetition rates. As-grown CdS QDs exhibited similar experimental phenomena when reducing laser repetition rates from 50 to 0.5 kHz. Decreasing the laser repetition rates can also apparently decrease the spin signals of the ν_1 component but have negligible effects on the ν_2 component. This suggests that the charging state of the ν_1 component is long-lived and subject to pile-up effects from previous pulses at high laser repetition rates. Decreasing the laser repetition rates decreases the pile-up effects. When pile-up effects are equal to or less important than the oxygen-induced electron removing, the ν_1 component disappears. The results in Figure 7 also imply that the charging state of the ν_2 component is short-lived and has no pile-up effects from previous pulses. The influence of laser repetition rates demonstrated here explains the fact that, in the literature, only one single Larmor frequency (corresponding to ν_2) was observed for pump–probe measurements with low laser repetition rates [7,25,26], while two Larmor frequencies were typically detected for the measurements with high laser repetition rates [5,13,22]. Accordingly, decreasing laser repetition rates is an effective way to isolate the spin signal of the ν_2 component. If a stronger spin signal of the ν_1 component is required, then high laser repetition rates must be used for the measurements.

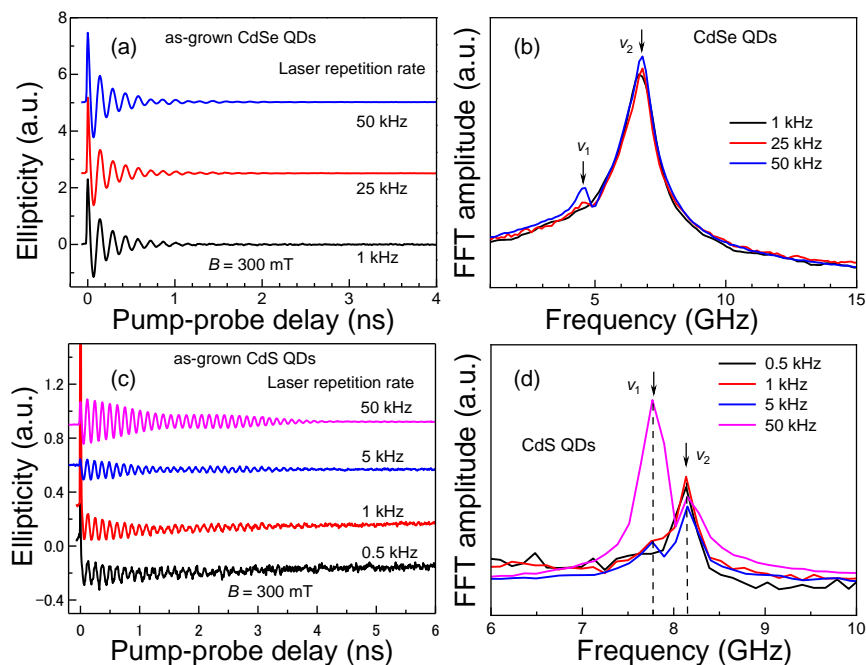


Figure 7. (a) Time-resolved ellipticity signals of CdSe QDs at laser repetition rates of 1, 25 and 50 kHz, respectively. (b) The corresponding FFT spectra of panel a. (c) Electron spin dynamics of CdS QDs with different laser repetition rates. (d) The corresponding FFT spectra of panel c.

For convenience, we summarize the methods that facilitate the acquisition of one single Larmor frequency, either the ν_1 or ν_2 component, in spin coherent measurements of our samples as follows:

- (1) Addition of an appropriate molar ratio of hole acceptors, Li[Et₃BH] or OT, in a N₂ atmosphere is beneficial to obtain the pure spin signal of the v_1 component.
- (2) Modifying colloidal QDs with an OT hole acceptor prepared in an air atmosphere provides advantages on the selection of the v_2 spin component.
- (3) Low laser repetition rates are convenient for the appearance of merely the v_2 component, whereas the spin signals of the v_1 component rise effectively when applying high laser repetition rates.

4. Conclusions

In conclusion, the coherent spin dynamics of CdSe and CdS colloidal QDs were studied using time-resolved ellipticity spectroscopy. Two spin components with different Larmor frequencies typically coexist in QDs with native ligands when measured at high laser repetition rates. In the presence of appropriate hole acceptors, e.g., Li[Et₃BH] and OT, with a proper molar ratio in N₂ or air atmosphere, the two spin components can be selectively enhanced or suppressed, leaving one pure spin component. Low laser repetition rates are beneficial to the appearance of the v_2 component solely. Higher laser repetition rates significantly contribute to the enhancement of the v_1 spin component. Consequently, those results imply that addition of hole acceptors either in an air or anaerobic atmosphere and adjusting laser repetition rates provide effective strategies to manipulate the spin signals in colloidal QDs, which is helpful for in-depth investigation of spin dynamics and practical applications.

Author Contributions: Conceptualization, T.J., Z.S. and D.F.; Data curation, M.J., Y.Z., R.H. and D.F.; Formal analysis, M.J., Y.Z. and R.H.; Investigation, M.J., Y.Z., R.H., Y.M., L.C. and P.L.; Writing—original draft, R.H. and D.F.; Writing—review and editing, R.H. and D.F. All authors have read and agreed to the published version of the manuscript.

Funding: This work was supported by the National Natural Science Foundation of China (Grants No 12174108, 91950112, 12104311, 12004239, 12074123 and 12034008).

Data Availability Statement: The data that support the findings of this study are available from the corresponding author upon reasonable request.

Conflicts of Interest: The authors declare no conflict of interest.

References

1. Loss, D.; DiVincenzo, D.P. Quantum Computation with Quantum Dots. *Phys. Rev. A At. Mol. Opt. Phys.* **1998**, *57*, 120–126. [[CrossRef](#)]
2. Awschalom, D.D.; Bassett, L.C.; Dzurak, A.S.; Hu, E.L.; Petta, J.R. Quantum Spintronics: Engineering and Manipulating Atom-Like Spins in Semiconductors. *Science* **2013**, *339*, 1174–1179. [[CrossRef](#)]
3. Hanson, R.; Awschalom, D.D. Coherent Manipulation of Single Spins in Semiconductors. *Nature* **2008**, *453*, 1043–1049. [[CrossRef](#)]
4. Khaetskii, A.V.; Nazarov, Y.V. Spin Relaxation in Semiconductor Quantum Dots. *Phys. Rev. B Condens. Matter Mater. Phys.* **2000**, *61*, 12639–12642. [[CrossRef](#)]
5. Gupta, J.A.; Awschalom, D.D.; Efros, A.L.; Rodina, A.V. Spin Dynamics in Semiconductor Nanocrystals. *Phys. Rev. B Condens. Matter Mater. Phys.* **2002**, *66*, 125307. [[CrossRef](#)]
6. Janßen, N.; Whitaker, K.M.; Gamelin, D.R.; Bratschitsch, R. Ultrafast Spin Dynamics in Colloidal ZnO Quantum Dots. *Nano Lett.* **2008**, *8*, 1991–1994.
7. Feng, D.H.; Li, X.; Jia, T.Q.; Pan, X.Q.; Sun, Z.R.; Xu, Z.Z. Long-Lived, Room-Temperature Electron Spin Coherence in Colloidal CdS Quantum Dots. *Appl. Phys. Lett.* **2012**, *100*, 122406. [[CrossRef](#)]
8. Biadala, L.; Shornikova, E.V.; Rodina, A.V.; Yakovlev, D.R.; Siebers, B.; Aubert, T.; Nasilowski, M.; Hens, Z.; Dubertret, B.; Efros, A.L.; et al. Magnetic Polaron on Dangling-Bond Spins in CdSe Colloidal Nanocrystals. *Nat. Nanotechnol.* **2017**, *12*, 569–574. [[CrossRef](#)]
9. Hu, R.R.; Wu, Z.; Zhang, Y.Y.; Yakovlev, D.R.; Liang, P.; Qiang, G.; Guo, J.X.; Jia, T.Q.; Sun, Z.R.; Bayer, M.; et al. Long-Lived Negative Photocharging in Colloidal CdSe Quantum Dots Revealed by Coherent Electron Spin Precession. *J. Phys. Chem. Lett.* **2019**, *10*, 4994–4999. [[CrossRef](#)]
10. Feng, D.H.; Yakovlev, D.R.; Pavlov, V.V.; Rodina, A.V.; Shornikova, E.V.; Mund, J.; Bayer, M. Dynamic Evolution from Negative to Positive Photocharging in Colloidal CdS Quantum Dots. *Nano Lett.* **2017**, *17*, 2844–2851. [[CrossRef](#)]

11. Hu, R.R.; Yakovlev, D.R.; Liang, P.; Qiang, G.; Chen, C.; Jia, T.Q.; Sun, Z.R.; Bayer, M.; Feng, D.H. Origin of Two Larmor Frequencies in the Coherent Spin Dynamics of Colloidal CdSe Quantum Dots Revealed by Controlled Charging. *J. Phys. Chem. Lett.* **2019**, *10*, 3681–3687. [[CrossRef](#)] [[PubMed](#)]
12. Li, X.; Feng, D.H.; Tong, H.F.; Jia, T.Q.; Deng, L.; Sun, Z.R.; Xu, Z.Z. Hole Surface Trapping Dynamics Directly Monitored by Electron Spin Manipulation in CdS Nanocrystals. *J. Phys. Chem. Lett.* **2014**, *5*, 4310–4316. [[CrossRef](#)] [[PubMed](#)]
13. Gupta, J.A.; Awschalom, D.D.; Peng, X.; Alivisatos, A.P. Spin Coherence in Semiconductor Quantum Dots. *Phys. Rev. B Condens. Matter Mater. Phys.* **1999**, *59*, R10421–R10424. [[CrossRef](#)]
14. Huxter, V.M.; Kovalevskij, V.; Scholes, G.D. Dynamics within the Exciton Fine Structure of Colloidal CdSe Quantum Dots. *J. Phys. Chem. B* **2005**, *109*, 20060–20063. [[CrossRef](#)] [[PubMed](#)]
15. Qiang, G.; Zhukov, E.A.; Evers, E.; Yakovlev, D.R.; Golovatenko, A.A.; Rodina, A.V.; Onushchenko, A.A.; Bayer, M. Electron Spin Coherence in CdSe Nanocrystals in a Glass Matrix. *ACS Nano* **2022**, *16*, 18838–18848. [[CrossRef](#)]
16. Yu, W.W.; Qu, L.; Guo, W.; Peng, X. Experimental Determination of the Extinction Coefficient of CdTe, CdSe, and CdS Nanocrystals. *Chem. Mater.* **2003**, *15*, 2854–2860. [[CrossRef](#)]
17. McArthur, E.A.; Morris-Cohen, A.J.; Knowles, K.E.; Weiss, E.A. Charge Carrier Resolved Relaxation of the First Excitonic State in CdSe Quantum Dots Probed with Near-Infrared Transient Absorption Spectroscopy. *J. Phys. Chem. B* **2010**, *114*, 14514–14520. [[CrossRef](#)]
18. Rinehart, J.D.; Schimpf, A.M.; Weaver, A.L.; Cohn, A.W.; Gamelin, D.R. Photochemical Electronic Doping of Colloidal CdSe Nanocrystals. *J. Am. Chem. Soc.* **2013**, *135*, 18782–18785. [[CrossRef](#)]
19. Zhang, Y.Y.; Jiang, M.Z.; Wu, Z.; Yang, Q.; Men, Y.M.; Cheng, L.; Liang, P.; Hu, R.R.; Jia, T.Q.; Sun, Z.R.; et al. Hyperfine-Induced Electron-Spin Dephasing in Negatively Charged Colloidal Quantum Dots: A Survey of Size Dependence. *J. Phys. Chem. Lett.* **2021**, *12*, 9481–9487. [[CrossRef](#)]
20. Wu, Z.; Zhang, Y.Y.; Hu, R.R.; Jiang, M.Z.; Liang, P.; Yang, Q.; Deng, L.; Jia, T.Q.; Sun, Z.R.; Feng, D.H. Hole-Acceptor-Manipulated Electron Spin Dynamics in CdSe Colloidal Quantum Dots. *J. Phys. Chem. Lett.* **2021**, *12*, 2126–2132. [[CrossRef](#)]
21. Stern, N.P.; Poggio, M.; Bartl, M.H.; Hu, E.L.; Stucky, G.D.; Awschalom, D.D. Spin Dynamics in Electrochemically Charged CdSe Quantum Dots. *Phys. Rev. B* **2005**, *72*, 161303(R). [[CrossRef](#)]
22. Fumani, A.K.; Berezovsky, J. Magnetic-Field-Dependent Spin Decoherence and Dephasing in Room-Temperature CdSe Nanocrystal Quantum Dots. *Phys. Rev. B Condens. Matter Mater. Phys.* **2013**, *88*, 155316. [[CrossRef](#)]
23. Schimpf, A.M.; Gunthardt, C.E.; Rinehart, J.D.; Mayer, J.M.; Gamelin, D.R. Controlling Carrier Densities in Photochemically Reduced Colloidal ZnO Nanocrystals: Size Dependence and Role of the Hole Quencher. *J. Am. Chem. Soc.* **2013**, *135*, 16569–16577. [[CrossRef](#)] [[PubMed](#)]
24. van Dijken, A.; Meulenkamp, E.A.; Vanmaekelbergh, D.; Meijerink, A. Influence of Adsorbed Oxygen on the Emission Properties of Nanocrystalline ZnO Particles. *J. Phys. Chem. B* **2000**, *104*, 4355–4360. [[CrossRef](#)]
25. Feng, D.H.; Shan, L.F.; Jia, T.Q.; Pan, X.Q.; Tong, H.F.; Deng, L.; Sun, Z.R.; Xu, Z.Z. Optical Manipulation of Electron Spin Coherence in Colloidal CdS Quantum Dots. *Appl. Phys. Lett.* **2013**, *102*, 062408. [[CrossRef](#)]
26. Zhang, Z.B.; Jin, Z.M.; Ma, H.; Xu, Y.; Lin, X.; Ma, G.H.; Sun, X.L. Room-Temperature Spin Coherence in Zinc Blende CdSe Quantum Dots Studied by Time-Resolved Faraday Ellipticity. *Phys. E Low-Dimens. Syst. Nanostructures* **2014**, *56*, 85–89. [[CrossRef](#)]

Disclaimer/Publisher’s Note: The statements, opinions and data contained in all publications are solely those of the individual author(s) and contributor(s) and not of MDPI and/or the editor(s). MDPI and/or the editor(s) disclaim responsibility for any injury to people or property resulting from any ideas, methods, instructions or products referred to in the content.